

Anti-tumor effect of miR-1291 in colorectal cancer

Jiaqi Wang

Department of Molecular Pathology, Division of Health Sciences, Graduate School of Medicine, Osaka University

Haruka Hirose

Department of Molecular Pathology, Division of Health Sciences, Graduate School of Medicine, Osaka University

Yuhki Yokoyama

Department of Molecular Pathology, Division of Health Sciences, Graduate School of Medicine, Osaka University

Yuki Shimomura

Department of Molecular Pathology, Division of Health Sciences, Graduate School of Medicine, Osaka University

Ryo Ikeshima

Department of Surgery, Gastroenterological Surgery, Graduate School of Medicine, Osaka University

Naoto Tsujimura

Department of Molecular Pathology, Division of Health Sciences, Graduate School of Medicine, Osaka University; Department of Surgery, Gastroenterological Surgery, Graduate School of Medicine, Osaka University

Saki Bonkobara

Department of Molecular Pathology, Division of Health Sciences, Graduate School of Medicine, Osaka University

Koki Takeda

Department of Surgery, Gastroenterological Surgery, Graduate School of Medicine, Osaka University

Tsuyoshi Hata

Department of Surgery, Gastroenterological Surgery, Graduate School of Medicine, Osaka University

Akira Inoue

Department of Molecular Pathology, Division of Health Sciences, Graduate School of Medicine, Osaka University; Department of Surgery, Gastroenterological Surgery, Graduate School of Medicine, Osaka University

Masayuki Hiraki

Department of Molecular Pathology, Division of Health Sciences, Graduate School of Medicine, Osaka University

Masahisa Ohtsuka

Department of Molecular Pathology, Division of Health Sciences, Graduate School of Medicine, Osaka University; Department of Surgery, Gastroenterological Surgery, Graduate School of Medicine, Osaka University

Naohiro Nishida

Department of Surgery, Gastroenterological Surgery, Graduate School of Medicine, Osaka University

Hidekazu Takahashi

Department of Surgery, Gastroenterological Surgery, Graduate School of Medicine, Osaka University

Naotsugu Haraguchi

Department of Surgery, Gastroenterological Surgery, Graduate School of Medicine, Osaka University

Shinji Tanaka

Department of Molecular Oncology, Department of Hepato-Biliary-Pancreatic Surgery, Graduate School of Medicine, Tokyo and Dental University

Xin Wu

Department of Molecular Pathology, Division of Health Sciences, Graduate School of Medicine, Osaka University

Susumu Tanaka

First Department of Oral and Maxillofacial Surgery, Graduate School of Dentistry, Osaka University

Masaki Mori

Department of Surgery, Graduate School of Medical Sciences, Kyushu University

Hirofumi Yamamoto (✉ hyamamoto@sahs.med.osaka-u.ac.jp)

Department of Molecular Pathology, Division of Health Sciences, Graduate School of Medicine, Osaka University <https://orcid.org/0000-0001-6959-9574>

Research article

Keywords: Colorectal cancer, miR-1291, DCLK1

Posted Date: November 20th, 2020

DOI: <https://doi.org/10.21203/rs.3.rs-41039/v2>

License: © ⓘ This work is licensed under a Creative Commons Attribution 4.0 International License.

[Read Full License](#)

Abstract

Background: MiR-1291 has an anti-tumor effect in carcinoma of kidney, esophagus, pancreas, and prostate. However, its role in colorectal cancer (CRC) has not been elucidated.

Methods: In this study, we explored the effect of miR-1291 in CRC cells (HCT116, DLD-1, and HT29) *in vitro*, and performed a tumor growth inhibitory assay in a mouse therapeutic model using DLD-1 cells. Flow cytometric analysis and Western blotting were performed to examine a role of miR-1291 in cell cycle regulation. We performed luciferase reporter assay to verify the interaction between DCLK1 and miR-1291 in HCT116 cells. Cancer stemness was evaluated by identifying the expression of BMI1 and CD133, as well as performing sphere formation assay.

Results: We found that miR-1291 significantly suppressed the proliferation, invasion, cell mobility, and colony formation capability of CRC cell lines. MiR-1291 caused altered expression of the cell cycle-regulatory proteins, representatively CDK inhibitors p21^{WAF1/CIP1} and p27^{KIP1} or CDK4. Moreover, intravenous administration of miR-1291 loaded on the super carbonate apatite delivery system significantly inhibited a tumor growth in the DLD-1 xenograft mouse model. A luciferase reporter assay showed that miR-1291 directly bound the 3' UTR sequence of DCLK1 and suppressed its expression at both the mRNA and protein levels in HCT116 expressing the DCLK1 protein. In addition, miR-1291 suppressed cancer stem cell (CSC) markers BMI1 and CD133 as well as sphere formation ability in HCT116 cells.

Conclusions: Taken together, these findings indicate that miR-1291 has an anti-tumor effect by modulating multiple functions, including cell cycle, invasiveness, and cancer stemness. Our data suggest that miR-1291 could be a promising nucleic acid medicine against CRC.

Background

Colorectal cancer (CRC) is the third most widespread cancer and the second most deadly cancer in the world. Approximately 1.8 million new cases of CRC and 881,000 related deaths were estimated in 2018 [1, 2]. In the past few decades, improved treatment options have become available, including surgery, radiotherapy, chemotherapy, and molecular-targeted therapy for advanced CRC [3-6]. However, the 5-year survival rate of CRC is <65% due to cancer relapse [2].

MicroRNAs (miRNAs) are short (18-25 nucleotides) internally originated non-coding RNAs that mainly bind to the 3'-untranslated region (3' UTR) of target mRNAs, contributing to mRNA cleavage or translational suppression [7, 8]. MiRNAs play an important role in many biological progresses, including tumor growth, apoptosis, invasion, and survival [9], which are closely related to oncogenesis and tumor progression. Recent studies have shown that the pathological mechanisms underlying CRC depend on a variety of signaling pathways, including Wnt/ β -catenin, EGFR, TGF- β , TP53, and epithelial-to-mesenchymal transition, and miRNAs play a pivotal role in regulating these pathways [10-12]. For example, miR-4689 has an anti-tumor effect on mutant KRAS CRC by inhibiting the EGFR pathway [13]. In

addition, miR-34a can inhibit cell proliferation and increase the expression of p21^{WAF1/CIP1} in HCT116 and RKO colorectal cancer cells [14].

Through *in silico* analysis and *in vitro* selection using doublecortin-like kinase 1 (DCLK1) as a target molecule (Supplementary Fig. S1a, b), we focused on miR-1291. DCLK1 is over-expressed in subsets of cancers and has an oncogenic function [15, 16]. In the Caki-2 renal cancer cell line, knocking down DCLK1 contributes to inhibition of cell proliferation, invasion, and wound-healing [17]. In 2013, DCLK1 was reported as a marker distinguishing tumor stem cells from intestinal normal stem cells [18]. Accumulating evidence supports the involvement of DCLK1 in the stemness of CRC [19, 20].

Cancer stem cells (CSCs) have distinct capability for self-renewal, unlimited proliferation, reduced capacity to undergo apoptosis, and multi-potential differentiation [21, 22]. Conventional anticancer drugs and radiotherapy may reduce tumor bulk, but CSCs can still survive, as they confer resistance to these therapies and cause distant metastases and recurrence in various cancers [23-25]. Thus, the development of CSC-targeted therapy may be an effective approach for overcoming the shortage of current therapies and completely cure CRC patients [26-28]. Several CSC markers for CRC have been found, including CD133, BMI1, and LGR5 [24, 29-30].

In recent years, miR-1291 has been demonstrated to have anti-tumor effects in carcinoma of the kidney, esophagus, pancreas, and prostate [31-34]. However, to the best of our knowledge, miR-1291 in CRC has not been reported. Therefore, we investigated the anti-tumor effect of miR-1291 in CRC cells in an effort to improve our understanding of the potential mechanisms of miR-1291 in CRC.

Methods

Cell lines and cell culture

Human CRC cell lines DLD-1, HT29, HCT116 were purchased from the American Type Culture Collection (Rockville, MD, USA). These cell lines were authenticated by morphological inspection, short tandem repeat profiling, and mycoplasma testing. DLD-1, HT29 cells were cultured in RPMI 1640 medium, and HCT116 cells were cultured in Dulbecco's modified Eagle's medium (DMEM), supplemented with 10% fetal bovine serum (FBS), 100 U/ml penicillin, and 100 µg/ml streptomycin. Cells were cultured in the humidified incubator at 37°C and 5% CO₂. All cells were passaged every 2 or 3 days.

Clinical tissue samples

Paired clinical tissue specimens (normal mucosa and colorectal cancer tissue) were collected from 20 patients who had surgery at Osaka University Hospital between 2016 and 2017. All tissue specimens were stored at -80 °C until RNA extraction. All patients gave written informed consent, in accordance with the guidelines approved by the Institutional Research Board of the institute. This study was conducted under the supervision of the Ethics Board of Osaka University Hospital.

MiRNA and plasmid transfection

Mimic-hsa-miR-1291 (miR-1291): sense (5'-UGGCCCUGACUGAAGACCAGCAGU-3') and antisense (5'-ACUGCUGGUCUUCAGUCAGGGCCA-3'), and negative control miR (miR-NC): sense (5'-AUCCGCGCGAUAGUACGUA-3') and antisense (5'-UACGUACUAUCGCGCGGAU-3'), were synthesized by Gene Design (Osaka, Japan). Cells were transfected with miRNAs and plasmids using Lipofectamine2000 (Thermo Fisher Scientific, Waltham, MA, USA) or Lipofectamine RNAiMAX (Thermo Fisher Scientific) according to the manufacturer's protocol.

RNA isolation

Total RNA was collected from cultured cells using TRIzol Reagent (Thermo Fisher Scientific) followed by phenol-chloroform extraction and ethanol precipitation. And miRNA was collected from tissue specimens and cultured cells using the miRNeasy kit (Qiagen, Hilden, Germany) according to the manufacturer's protocol. Total RNA concentration and purity were measured using a NanoDrop one spectrophotometer (Thermo Fisher Scientific), at 260 and 280 nm ($A_{260/280}$) wavelengths.

Quantitative real-time PCR analysis of messenger RNA

A High Capacity cDNA Reverse Transcription Kit (Thermo Fisher Scientific) was used to synthesize the complementary DNA from 2.5 μ g of total RNA according to the manufacturer's instructions. The quantitative real-time PCR (qRT-PCR) for DCLK1, BMI1 and CD133 RNA were performed using was amplified using oligonucleotide primers and the LightCycler 480 Real-Time PCR system (Roche, Basel, Switzerland). The amplification products were detected using the THUNDERBIRD SYBR qPCR Mix (TOYOBO, Osaka, Japan), and the level of target gene expression was calculated. The qRT-PCR conditions were 95°C for 30 sec; 40 cycles of 95°C for 10 sec, and 60°C for 10 sec, 72°C for 30 sec. The expression of the target gene was normalized to endogenous GAPDH expression. Relative expression was quantified by the $2^{-\Delta\Delta C_t}$ method. The PCR primers are listed in Supplementary Table S1.

Quantitative real-time PCR analysis of miR-1291 and miR-NC

We used the TaqMan MicroRNA Reverse Transcription Kit (Thermo Fisher Scientific) to synthesize the complementary DNA from 25ng of total RNA according to the manufacturer's protocol. The qRT-PCR of miRNA was then performed using TaqMan Universal PCR Master Mix, No AmpErase UNG (Thermo Fisher Scientific) with a 7900 HT Sequence Detection System (Thermo Fisher Scientific). RNU6B was used as the endogenous control. The qRT-PCR conditions were 95°C for 10 min; 45 cycles of 95°C for 15 sec, and 60°C for 1 min, 72°C for 1 sec; cooling to 40°C for 30 sec. Relative expression was quantified with the $2^{-\Delta\Delta C_t}$ method.

Proliferation assay

Cells were seeded in 96-well plates at a density of 4000-8000 per well and were transfected with miR-NC or miR-1291 at a final concentration of 30 nM the second day after seeding. Twenty-four, 48, and 72

hours after transfection, 10 μ l of Cell Counting Kit-8 (DOJINDO Molecular technologies, Inc., Kumamoto, Japan) was added to each well, and the 96-well plates were shaded for 2 hours. After that, the absorbance was detected by Multiskan Go (Thermo Fisher Scientific), and the subtraction difference of absorbance between wavelength of 630 nm and 450 nm was used to determine cell number.

Matrigel invasion assay

Cells were seeded in BD BioCoat Matrigel Invasion Chambers (BD Biosciences, San Jose, CA, USA) at a density of 50,000-100,000 cells per chamber. The cells were transfected with the miRNAs at a final concentration of 50 nM. After 48-72 h of transfection, invaded cells were fixed with 10% formalin and then stained with hematoxylin for counting.

Wound healing assay

Cells were seeded in ibidi culture 2-well inserts (ibidi, Gräfelfing, Germany) in 24-well plates at a confluent density. The inserts were removed after 24 hours to create wounds. The miRNAs were transfected at a final concentration of 30 nM. At 0-48 hours after transfection, the areas of the wounds were measured using ImageJ software.

Colony formation assay

Cells were seeded in a 6-well plate at a density of 1×10^5 cells per well, incubated overnight, and then transfected with miR-NC or miR-1291 at a final concentration of 30 nM for 8 hours and then reseeded in 6-well plates at a density of 500 cells per well. After 10 days, the cells were fixed with methanol and stained by crystal violet for counting.

Cell cycle assay

Cells were starved in serum-free medium for 48 hours. Twenty-four hours before the end of starvation, miR-NC or miR-1291 was transfected at a final concentration of 30~40 nM. Cells were collected at the indicated times (0, 12, 24, 48 hours), fixed in 70% ethanol for 30 minutes at 4°C. After fixation, cells were washed twice with PBS and incubated with RNase (Sigma Aldrich, St. Louis, MO, USA) for 20 minutes at 37°C. Cells were treated with PI (Dojindo) for 20 minutes on ice and analyzed by flow cytometry (Spectral Analyzer SA3800, Sony Biotechnology, Inc., Tokyo, Japan).

Western blot analysis

Cells were seeded in 6-well plates at a density of 100,000-200,000 per well and then transfected with miR-NC or miR-1291 at a final concentration of 30~50 nM the next day. After 48 and 72 hours, cells were rinsed twice with PBS and lysed with RIPA buffer (0.05 M Tris-HCl pH 7.6, 0.15 M NaCl, 1% Nonidet P40, 0.5% sodium deoxycholate, 0.1% SDS) with 1% proteinase inhibitor cocktail (Nacalai Tesque, Kyoto, Japan). The protein samples were electrophoresed by sodium dodecyl sulfate-polyacrylamide gel electrophoresis (SDS-PAGE) and transferred to a polyvinylidene fluoride transfer membrane (PVDF, Bio-

Rad, Hercules, CA, USA). The membranes were incubated with primary antibodies, including anti-ACTB ((13E5) Rabbit mAb #4970, Cell Signaling Technology, Danvers, MA, USA), and anti-DCLK1 (ab31704, Abcam, Cambridge, UK), anti-BMI1 (10832-1-AP, Thermo Fisher Scientific), anti-p21^{WAF1/CIP1} (ab80633, Abcam), anti-p27^{KIP1} (sc-528, Santa Cruz Biotechnology, Dallas, TX, USA), anti-CDC25A (#3652, Cell Signaling Technology), anti-CDC25B (#9525, Cell Signaling Technology), anti-CDC25C ((5H9) Rabbit mAb #4688, Cell Signaling Technology), anti-CDK4 (MAB8879, Merck Millipore, Burlington, MA, USA), anti-CDK6 (SAB4300596, Sigma-Aldrich), anti-Cyclin D1 (#2922, Cell Signaling Technology), anti-Cyclin E1 (sc-247, Santa Cruz Biotechnology), anti-Rb (ab24, Abcam). HRP anti-mouse IgG antibody (NA931, GE Health Care, Little Chalfont, UK) and anti-rabbit IgG antibody (NA934, GE Health Care) were used as secondary antibodies. The bands were visualized by the ECL Detection System (GE Health Care).

pmirGLO plasmid vector construction

The 3' UTR of DCLK1 mRNA was amplified by PCR using the following primer sequences (amplified product size 211 bp): Forward 5'-GCTCGCTAGCCTCGAGCTAGTGTACTGAGCCTGCGG-3', Reverse 5'-ATGCCTGCAGGTCGACTGACTGGTCACATTCCACTG-3'. The amplified products were subcloned and ligated into the multicloning site between Sal I and Xho I in the pmirGLO Dual-Luciferase miRNA Target Expression Vector (Promega, Madison, WI, USA) using the In-Fusion HD Cloning Kit (Clontech, Mountain View, CA). The vectors with mismatched 3' UTR sequences were constructed using the QuikChange Site Directed Mutagenesis Kit (Agilent Technologies, Santa Clara, CA, USA) according to the manufacturer's protocol. The PCR primers for mutated type and deleted type plasmids are listed in Supplementary Table S1. The entire sequence (insert and vector) was confirmed by Sanger sequencing.

Luciferase reporter assay

Cells were seeded in 96-well plates at a density of 10,000 cells per well and co-transfected with 50 ng of the DCLK1 wild type (WT) or 2-nucleotide mutated (Mut) or 3-nucleotide deleted (Del) 3' UTR reporter vectors, and 50 nM of either miR-1291 mimics or miR-NC using Lipofectamine 2000 according to the manufacturer's protocol. After 24 hours of transfection, cells were lysed and measured for both firefly and renilla luciferase activity using the Dual-Luciferase Reporter Assay System (Promega) according to the manufacturer's protocol.

Sphere formation assay

HCT116 cells were seeded in a 6-well plate at a density of 1×10^5 cells per well, incubated overnight, and transfection with miR-NC or miR-1291 at a final concentration of 50 nM. Then after 24 hours of transfection single cells were reseeded in 96-Well Clear Ultra Low Attachment Microplates (Corning Inc., Corning, NY, USA) at the density of 1,000 cells per well. And the cells were cultured in DMEM/F-12 serum-free medium (Thermo Fisher Scientific) supplemented with 20 ng/ml epithelial growth factor, 10 ng/ml basic fibroblast growth factor-2 (PeproTech, Cranbury, NJ, USA), and 100 U/ml penicillin, and 100 µg/ml streptomycin. Cells were cultured in the humidified incubator at 37°C and 5% CO₂. The number of spheres ≥ 40 µm was counted 4 days after reseeded.

Flow cytometric analysis for CD133 marker expression

HCT116 cells were seeded in a 6-well plate at a density of 1×10^5 cells per well, incubated overnight, and transfection with miR-NC or miR-1291 at a final concentration of 50 nM. After 48 hours of transfection the cells were resuspended and one million cells were incubated with antibodies against human CD133 (APC-conjugated, No. 130-113-106, Miltenyi Biotec, Bergisch Gladbach, Germany) at the concentration of 1: 50 on ice for 20 minutes in the dark, centrifuged, and washed twice with PBS containing 2% FBS. Spectral Analyzer (SA3800, Sony Biotechnology, Inc.) was used for flow cytometric analyses. Dead cells were excluded by utilizing forward and side scatter.

In vivo therapeutic model

DLD-1 cells were mixed with Matrigel (BD Biosciences) and medium at a 1:1 ratio (vol: vol). Approximately 2×10^6 cells in 100 μ L medium/Matrigel solution were injected subcutaneously into both sides of the lower back regions of 4-week-old female nude mice (NIHON CLEA, Tokyo, Japan). The mice were divided randomly into a parent group (n=5), a miR-NC group (n=6) and a miR-1291 group (n=6) for evaluation of anti-tumor growth effects and safety. After tumor volumes reached 80 mm³, we intravenously administered formulated miRNA with super carbonate apatite as the vehicle via the tail vein at a dose of 40 μ g per injection [13, 35-40]. Mice were treated eight times with formulated miR-NC or miR-1291 over 2 weeks. Tumor volumes were determined as previously described [13, 35-40]. The animal facility was SPF and was kept at 20–24 °C. The dark/light cycle was 12/12 hours. All animal experiments were performed in accordance with currently prescribed guidelines, including the Animal (Scientific Procedures) Act 1986, and following a protocol approved by Osaka University.

Statistical analysis

Data are presented as the mean \pm SEM. Statistical analyses were performed using GraphPad Prism 5 (San Diego, CA, USA) and Microsoft Excel. The statistical differences between the miR-NC and miR-1291 groups were analyzed by student's t-test (two-tailed). The expression levels of miRNAs in normal and cancer colorectal tissues were analyzed using the Wilcoxon signed-rank test. *In vivo* tumor growth was analyzed with one-way ANOVA followed by Bonferroni's multiple comparisons test. $P < 0.05$ was considered significant.

Results

Expression of miR-1291 in CRC cells and clinical tissue specimens

We evaluated the expression of miR-1291 in CRC cell lines and non-tumor human HEK293 cells by qRT-PCR (Supplementary Fig. S2a). We then compared the expression level of miR-1291 in normal mucosa and CRC cancer tissues from 20 paired clinical tissue specimens. Although the tumor tissues tended to express generally low miR-1291 expression, statistical difference was not noted between normal colonic mucosa and CRC tissues (Supplementary Fig. S2b).

MiR-1291 overexpression after transfection

Either 4 hours or 24 hours after transfection of miRNAs, miR-1291 transfection group presented 1,000 to 5,000-fold higher miR-1291 expression than miR-NC transfection group in DLD-1, HT29, and HCT116 cells (Fig. 1a).

MiR-1291 inhibited cell proliferation

To confirm the anti-tumor effect of miR-1291 in CRC cell growth, we detected the absorbance of cells transfected with miR-NC or miR-1291 as determined by Cell Counting Kit-8. The miR-1291 transfection group presented a significant low absorbance compared to the miR-NC transfection group in DLD-1, HT29, and HCT116 cells after 48 and 72 hours of transfection (Fig. 1b). MiR-1291 significantly suppressed the proliferation ability of the three cell lines.

MiR-1291 inhibited cell invasion

MiR-NC or miR-1291 was transfected into CRC cells to evaluate the effect on invasion ability. The cells invading through Matrigel were stained with hematoxylin 48 hours for DLD-1 or 72 hours for HT29 and HCT116 after transfection and then counted. The invasion ability of miR-1291-transfected cells was significantly inhibited compared to miR-NC transfected cells in the three cell lines tested (Fig. 1c).

MiR-1291 inhibited cell migration ability

We evaluated the effect of miR-1291 on the wound-healing ability of CRC cells. The wound area of the cells was measured at the same location every 24 hours after miR transfection. The migration ability of DLD-1, HT29, and HCT116 cells was significantly suppressed in the miR-1291 group compared to miR-NC group either at 24 hours or 48 hours or both (Fig. 2a).

MiR-1291 inhibited colony formation ability

To confirm the function of miR-1291 in cell colony formation ability, we observed and evaluated the colony formation of the CRC cells which were transfected with miR-NC or miR-1291. The colonies were stained with crystal violet 10 days after transfection, and we counted the number of the colonies. MiR-1291 significantly inhibited the colony formation potential compared to miR-NC in DLD-1, HT29, and HCT116 cells (Fig. 2b).

Altered expression of cell cycle components by treatment of miR-1291

Cells were examined for the change in cell cycle regulatory protein expression after transfection of miR-1291 in the standard medium supplemented with FBS. In DLD-1 cells, the expression of CDK inhibitors p21^{WAF1/CIP1} and p27^{KIP1} were up-regulated and CDK4 and CDC25A level decreased at 48 hours after transfection with treatment of miR-1291 (Fig. 3a). In HT29 cells, the expression of p21^{WAF1/CIP1} and p27^{KIP1} protein increased at 48 hours compared to miR-NC group (Fig. 3a). In HCT116

cells, transfection of miR-1291 up-regulated the expression of p21^{WAF1/CIP1} and p27^{KIP1}, down-regulated the expression of CDK4, compared to miR-NC cells (Fig. 3a). We then examined the cell cycle distribution after serum starvation (Supplementary Fig. S3a, b; Time points: 0, 12, 24, and 24 hours). Twelve hours refed with FBS, cells in G1 phase were significantly increased in miR-1291 treated cultures of DLD-1 cells (60.81% vs 67.89%, Fig. 3b). However, cell population in each cell cycle phase was not apparently changed in HT29 cells throughout the time points examined (Fig. 3b, Supplementary Fig. S3b). MiR-1291 increased the percentage of cells in G2/M phase in HCT116 cells compared to miR-NC after 24 hours of addition of serum to the starved cells (26.35% vs 33.15%, Fig. 3b).

Anti-tumor effects of miR-1291 *in vivo*

We used a DLD-1 tumor xenograft mouse model to verify the anti-tumor effect of miR-1291 *in vivo*. Compared to miR-NC group and no treatment group, systemic administration of miR-1291 on super carbonate apatite significantly inhibited the growth of tumor (Fig. 4a). No obvious body weight loss of mice was observed among the three groups (Fig. 4b).

MiR-1291 directly targeted DCLK1

We performed luciferase reporter assays to confirm whether miR-1291 directly bind to DCLK1. In HCT116 cells, co-transfection with miRNA-1291 significantly inhibited the luciferase activity of wild type of DCLK1-3' UTR reporter vector, compared to miR-NC (** $P < 0.01$). On the other hand, no significant difference in luciferase activity was noted between miR-1291 group and miR-NC group in use of 2-nucleotide mutated type (Mut) or 3-nucleotide deleted type (Del) DCLK1-3' UTR reporter vector (Fig. 5a, b). Transfection with miR-1291 significantly suppressed the expression of DCLK1 at both the mRNA (Fig. 5c) and protein levels (Fig. 5d, Supplementary Fig. S4) compared to miR-NC. In miR-1291 treated group, the protein expression of DCLK1 was reduced to 30.6% of that treated with miR-NC (Fig. 5d). These findings indicate that DCLK1 is a direct target of miR-1291 in HCT116.

MiR-1291 suppressed stem-like properties in HCT116 cells

Our previous study showed that HCT116, but not DLD-1 and HT29 expressed DCLK1 [16], therefore, we assessed stemness of HCT116 cells after treatment of miR-1291. We demonstrated that other CSC markers in addition to DCLK1, including BMI1 and CD133, were significantly down-regulated by miR-1291 overexpression at mRNA level (Fig. 6a, b). MiR-1291 treatment also down-regulated the protein level of BMI1 by Western blot analysis (Fig. 6c). Moreover, the ratio of CD133 positive cells decreased with treatment of miR-1291 by flow cytometric analysis (Fig. 6d). Furthermore, miR-1291 treatment significantly decreased the ability of sphere formation in HCT116 cells (Fig. 6e). These findings suggest that miR-1291 may be involved in the regulation of stem cell properties through direct inhibition of DCLK1 in HCT116.

Discussion

MicroRNA is emerging as a next generation cancer treatment [41-44]. Studies showed that miR-1291 had anti-tumor effects in multiple cancers including renal cancer, esophagus cancer, pancreatic cancer, and prostate cancer [31-34]. However, to the best of our knowledge, there is no report of miR-1291 in CRC which is one of the widespread cancers in the world. In this study, we clearly demonstrated that miR-1291 exhibited anti-tumor effects in HCT116, DLD-1, and HT29 CRC cells in terms of cell proliferation, invasion, cell mobility, colony-forming abilities, and cell cycle regulation. Moreover, intravenous administration of miR-1291 loaded on the super apatite delivery system significantly inhibited *in vivo* tumor growth compared with miR-NC treated group.

In this study we started to select miRNAs using doublecortin-like kinase 1 (DCLK1) as a target [18, 45] as well as Notch and Wnt signaling (Supplementary Fig. S1). DCLK1 belongs to the protein kinase superfamily and the doublecortin family, and is over-expressed in several human malignancies, including colorectal, pancreas, kidney, and prostate cancer [46-49]. Excision of DCLK1-positive CSCs results in regression of the intestinal tumor without apparent impairment of normal tissue, which indicates that DCLK1 may be a novel target for CSC-targeted therapy [18]. Screening with ODC degron-transduced cells revealed that miR-1291 inhibited both CSC and non-CSC. Although degron (+) cells were more resistant to miR-1291 treatment compared with degron (-) cells, its growth inhibitory effect was even stronger than that given by a putative Onco-miR, miR-34a. Targeting both CSC and non-CSC by miR-1291 could be attributed to the feature of miRNA that can bind to multiple molecules.

We recently reported that sh DCLK1 clones, in which DCLK1 expression was silenced by short hairpin DCLK1 RNA, exhibited decreased cell growth, invasion, migration abilities and EMT in HCT116 [16]. Other investigators also showed that DCLK1 level was tightly associated with spheroid formation in HCT116, which is a hallmark for CSC [50, 51]. In this study, we verified that miR-1291 directly bound to the 3' UTR of the DCLK1 mRNA sequence, leading to decreased expression of DCLK1 at both the mRNA and protein levels. In addition to DCLK1, miR-1291 lowered BMI1 and CD133 expression, which are also representative CSC markers in CRC. Moreover, we confirmed that miR-1291 inhibited sphere formation ability of HCT116 cells. These results support the notion that miR-1291 suppresses the cancer stemness through direct targeting DCLK1, suggesting that miR-1291 may be a novel CSC-targeted therapeutic strategy for CRC.

On the other hand, DLD-1 and HT29 cells which did not express DCLK1 [16] also exerted the potent tumor inhibitory effects, suggesting that certain other mechanism should be operating in these CRC cells and it may suppress non-stem cells. With this regard, studies reported that miR-1291 regulates SLC2A1/GLUT1 in A498 and 786-O renal cancer cells [31], MUC1 in human esophagus cancer EC9706 and EC-1 cells [32], the forkhead box protein A2-anterior gradient 2 (FOXA2-AGR2) pathway in PANC-1 pancreatic cancer cells [33]. Furthermore, miR-1291 has been shown to inhibit cell growth and tumorigenesis in prostate cancer by binding to MED1 [34]. These molecules as well as other targets should be further explored.

One of the major effects observed by miR-1291 treatment was drastic change in the cell cycle components. Western blot analysis showed increase in p21^{WAF1/CIP1} and p27^{KIP1} in the three CRC cell

lines at 48 hours. These CDK inhibitors bind to and block the G1-S accelerators Cyclin D1-CDK4/6 complex and Cyclin E1-CDK2 complex, leading to restraint from the G1 to S phase [52-54]. We also found that CDK4 decreased in DLD-1 and HCT116. Under the condition supplemented with FBS we could not observe obvious change in the cell cycle distribution between miR-NC and miR-1291 treatment. Time course study after serum starvation revealed the delay in G1-S transition at 12 hours in DLD-1 and the delay in G2-M transition at 24 hours in HCT116. Collectively these results suggest that miR-1291 could cause dysregulation of cell cycle control even though its effectual action point and timing may differ by cell types. In terms of the association of cell cycle regulators with DCLK1, Chandrakesan *et al.* reported that DCLK1-positive cells had higher expression of p21^{WAF1/CIP1} and p27^{KIP1} and maintained quiescence in normal small intestine [55]. However, the current study demonstrated that miR-1291 inhibited DCLK1 and up-regulated p21^{WAF1/CIP1} and p27^{KIP1} which may cause G1 phase arrest. When we examined expression of these CDK inhibitors using the sh DCLK1 clones, p27^{KIP1} level increased (Supplementary Fig. S5a, b). These findings may partially help to explain an opposite role of DCLK1 in the cell cycle between normal and cancer cells.

Conclusions

In conclusion, miR-1291 presented a strong anti-tumor effect on CRC cells and played an important role in both delaying the cell cycle and suppressing cancer stemness. To the best of our knowledge, this is the first study that demonstrates the function of miR-1291 in CRC. Considering the anti-tumor effect of miR-1291 in the broad range of cancer type [31-34], this microRNA may be one of the candidates for the next generation nucleic acid medicine using the practical DDS systems [11, 12, 35, 43, 44].

Declarations

Ethics approval and consent to participate: This study was performed in accordance with the Declaration of Helsinki and the study was approved by the Ethics Board of Osaka University (approval No. 13377-5; Osaka, Japan).

Consent for publication: All patients gave written informed consent, in accordance with the guidelines approved by the Institutional Research Board of the institute.

Availability of data and materials: None.

Competing interests: The authors have no competing interests to declare.

Funding: This work was supported by a grant from Kagoshima Shinsangyo Sousei Investment Limited Partnership (its general partner is Kagoshima Development Co., Ltd) and by Grant-in-Aid for Young Scientists (B), JSPS KAKENHI (No.18K16361).

for data collection.

Authors' contributions: All authors have read and approved the manuscript. Conceptualization, H.Y. and M.M.; Supervision, H.Y., M.M., H.T., H.H.; methodology, X.W., Y.Y., N.T., N.H, Sh.T.; validation, M.H., M.O.; investigation, J.W., S.B., H.H., X.W. R.I.,Y.S, Su T; software, K.T.; writing-original draft, J.W.; review and editing, A.I., H.Y., T.H., N.N.

Acknowledgements: We are grateful to Satoshi Shibata, Masaaki Miyo, and Yamin Qian, for editing this manuscript.

Abbreviations

Abbreviation	Definition
CRC	colorectal cancer
CSC	cancer stem cell
miRNA	microRNA
3' UTR	3'-untranslated region
DCLK1	doublecortin-like kinase 1
DMEM	dulbecco's modified Eagle's medium
FBS	fetal bovine serum
miR-1291	mimic-hsa-miR-1291
miR-NC	negative control miR
qRT-PCR	quantitative real-time PCR
WT	Wild type
Mut	Mutated type
Del	Deleted type
FOXA2-AGR2	forkhead box protein A2-anterior gradient 2
sCA	super carbonate apatite
ODC	ornithine decarboxylase
Gdeg	ZsGreen-degron ODC
miR-34a	mimic-hsa-miR-34a-5p

References

1. Bray F, Ferlay J, Soerjomataram I, Siegel RL, Torre LA, Jemal A. Global cancer statistics 2018: GLOBOCAN estimates of incidence and mortality worldwide for 36 cancers in 185 countries. *CA Cancer J Clin.* 2018; doi: 10.3322/caac.21492.
2. Rawla P, Sunkara T, Barsouk A. Epidemiology of colorectal cancer: incidence, mortality, survival, and risk factors. *Prz Gastroenterol.* 2019; doi: 10.5114/pg.2018.81072.
3. Kobayashi H, Mochizuki H, Morita T, Kotake K, Teramoto T, Kameoka S, et al. Characteristics of recurrence after curative resection for T1 colorectal cancer: Japanese multicenter study. *J Gastroenterol.* 2011; doi: 10.1007/s00535-010-0341-2.
4. Brenner H, Kloor M, Pox CP. Colorectal cancer. *Lancet.* 2014; doi: 10.1016/S0140-6736(13)61649-9.
5. Watanabe T, Muko K, Hashiguchi Y, Ito Y, Saito Y, Hamaguchi T, et al. Japanese Society for Cancer of the Colon and Rectum (JSCCR) guidelines 2016 for the Treatment of Colorectal Cancer. *Int J Clin Oncol.* 2018; doi: 10.1007/s10147-017-1101-6.
6. Janet S Graham & James Cassidy. Adjuvant therapy in colon cancer. *Expert Rev of Anticancer Ther.* 2012; doi: 10.1586/era.11.189.
7. Fischer SEJ. RNA Interference and MicroRNA-Mediated Silencing. *Curr Protoc Mol Biol.* 2015; doi: 10.1002/0471142727.mb2601s112.
8. Iwakawa HO, Tomari Y. The Functions of MicroRNAs: mRNA Decay and Translational Repression. *Trends Cell Biol.* 2015; doi: 10.1016/j.tcb.2015.07.011.
9. Kunz M, Göttlich C, Walles T, Nietzer, Dandekar G, Dandekar T. MicroRNA-21 versus microRNA-34: Lung cancer promoting and inhibitory microRNAs analysed in silico and in vitro and their clinical impact. *Tumour Biol.* 2017; doi: 10.1177/1010428317706430.
10. Rahmani F, Avan A, Hashemy SI, Hassanian SM. Role of Wnt/beta-catenin signaling regulatory microRNAs in the pathogenesis of colorectal cancer. *J Cell Physiol.* 2018; doi: 10.1002/jcp.25897.
11. To KK, Tong CW, Wu M, Cho WC. MicroRNAs in the prognosis and therapy of colorectal cancer: From bench to bedside. *World J Gastroenterol.* 2018; doi: 10.3748/wjg.v24.i27.2949.
12. Chi Y, Zhou D. MicroRNAs in colorectal carcinoma—from pathogenesis to therapy. *J Exp Clin Cancer Res.* 2016; doi: 10.1186/s13046-016-0320-4.
13. Hiraki M, Nishimura J, Takahashi H, Wu X, Takahashi Y, Miyo M, et al. Concurrent Targeting of KRAS and AKT by MiR-4689 Is a Novel Treatment Against Mutant KRAS Colorectal Cancer. *Mol Ther Nucleic Acids.* 2015; doi: 10.1038/mtna.2015.5.
14. Tazawa H, Tsuchiya N, Izumiya M, Nakagama H. Tumor-suppressive miR-34a induces senescence-like growth arrest through modulation of the E2F pathway in human colon cancer cells. *Proc Natl Acad Sci U S A.* 2007; doi: 10.1073/pnas.0707351104.
15. Chandrakesan P, Yao J, Qu D, May R, Weygant N, Ge Y, et al. Dclk1, a Tumor Stem Cell Marker, Regulates Pro-Survival Signaling and Self-Renewal of Intestinal Tumor Cells. *Mol Cancer.* 2017; doi: 10.1186/s12943-017-0594-y.

16. Makino S, Takahashi H, Okuzaki D, Miyoshi N, Haraguchi N, Hata T, et al. DCLK1 integrates induction of TRIB3, EMT, drug resistance and poor prognosis in colorectal cancer. *Carcinogenesis*. 2019; doi: 10.1093/carcin/bgz157.
17. Weygant N, Qu D, May R, Tierney RM, Berry WL, Zhao L, et al. DCLK1 Is a Broadly Dysregulated Target Against Epithelial-Mesenchymal Transition, Focal Adhesion, and Stemness in Clear Cell Renal Carcinoma. *Oncotarget*. 2015; doi: 10.18632/oncotarget.3059.
18. Nakanishi Y, Seno H, Fukuoka A, Ueo T, Yamaga Y, Maruno T, et al. Dclk1 distinguishes between tumor and normal stem cells in the intestine. *Nat Genet*. 2013; doi: 10.1038/ng.2481.
19. Chandrakesan P, Weygant N, May R, Qu D, Chinthalapally HR, Sureban SM, et al. DCLK1 Facilitates Intestinal Tumor Growth via Enhancing Pluripotency and Epithelial Mesenchymal Transition. *Oncotarget*. 2014; doi: 10.18632/oncotarget.2393.
20. Liu W, Wang S, Sun Q, Yang Z, Liu M, Tang H. DCLK1 Promotes Epithelial-Mesenchymal Transition via the PI3K/Akt/NF- κ B Pathway in Colorectal Cancer. *Int J Cancer*. 2018; doi: 10.1002/ijc.31232.
21. Plaks V, Kong N, Werb Z. The cancer stem cell niche: how essential is the niche in regulating stemness of tumor cells? *Cell Stem Cell*. 2015; doi:10.1016/j.stem.2015.02.015.
22. Ayob AZ, Ramasamy TS. Cancer stem cells as key drivers of tumour progression. *J Biomed Sci*. 2018; doi: 10.1186/s12929-018-0426-4.
23. Zhao J. Cancer stem cells and chemoresistance: The smartest survives the raid. *Pharmacol Ther*. 2016; doi: 10.1016/j.pharmthera.2016.02.008.
24. de Sousa e Melo F, Kurtova AV, Harnoss JM, Kljavin N, Hoeck JD, Hung J, et al. A distinct role for Lgr5⁺ stem cells in primary and metastatic colon cancer. *Nature*. 2017; doi: 10.1038/nature21713.
25. Vermeulen L, Todaro M, de Sousa Mello F, Sprick MR, Kemper K, Perez Alea M, et al. Single-cell cloning of colon cancer stem cells reveals a multi-lineage differentiation capacity. *Proc Natl Acad Sci U S A*. 2008; doi: 10.1073/pnas.0805706105.
26. Szaryńska M, Olejniczak A, Kobiela J, Sychalski P, Kmiec Z. Therapeutic strategies against cancer stem cells in human colorectal cancer (Review). *Oncol Lett*. 2017; doi: 10.3892/ol.2017.7261.
27. Vermeulen L, Sprick MR, Kemper K, Stassi G, Medema JP. Cancer stem cells – old concepts, new insights. *Cell Death Differ*. 2008; doi: 10.1038/cdd.2008.20.
28. Clarke MF, Dick JE, Dirks PB, Eaves CJ, Jamieson CH, Jones DL, et al. Cancer Stem Cells— Perspectives on Current Status and Future Directions: AACR Workshop on Cancer Stem Cells. *Cancer Res*. 2006; doi: 10.1158/0008-5472.CAN-06-3126.
29. Ren F, Sheng WQ, Du X. CD133: a cancer stem cells marker, is used in colorectal cancers. *World J Gastroenterol*. 2013; doi: 10.3748/wjg.v19.i17.2603.
30. Soheilifar MH, Moshtaghian A, Maadi H, Izadi F, Saidijam M. BMI1 Roles in Cancer Stem Cells and Its Association with MicroRNAs Dysregulation in Cancer: Emphasis on Colorectal Cancer. *Int J Cancer Manag*. 2018; doi: 10.5812/ijcm.82926.

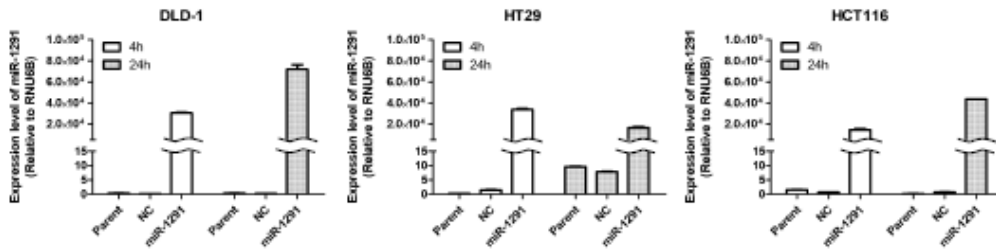
31. Yamasaki T, Seki N, Yoshino H, Itesako T, Yamada Y, Tatarano S, et al. Tumor-suppressive microRNA-1291 Directly Regulates Glucose Transporter 1 in Renal Cell Carcinoma. *Cancer Sci.* 2013; doi: 10.1111/cas.12240.
32. Luo H, Guo W, Wang F, You Y, Wang J, Chen X, et al. miR-1291 Targets Mucin 1 Inhibiting Cell Proliferation and Invasion to Promote Cell Apoptosis in Esophageal Squamous Cell Carcinoma. *Oncol Rep.* 2015; doi: 10.3892/or.2015.4206.
33. Tu MJ, Pan YZ, Qiu JX, Kim EJ, Yu AM. MicroRNA-1291 targets the FOXA2-AGR2 pathway to suppress pancreatic cancer cell proliferation and tumorigenesis. *Oncotarget.* 2016; doi: 10.18632/oncotarget.9999.
34. Cai Q, Zhao A, Ren L, Chen J, Liao K, Wang Z, Zhang W. MicroRNA-1291 Mediates Cell Proliferation and Tumorigenesis by Downregulating MED1 in Prostate Cancer. *Oncol Lett.* 2019; doi: 10.3892/ol.2019.9980.
35. Wu X, Yamamoto H, Nakanishi H, Yamamoto Y, Inoue A, Tei M, et al. Innovative delivery of siRNA to solid tumors by super carbonate apatite. *PLoS One.* 2015; doi: 10.1371/journal.pone.0116022.
36. Ogawa H, Wu X, Kawamoto K, Nishida N, Konno M, Koseki J, et al. MicroRNAs Induce Epigenetic Reprogramming and Suppress Malignant Phenotypes of Human Colon Cancer Cells. *PLoS One.* 2015; doi: 10.1371/journal.pone.0127119.
37. Takeyama, H., Yamamoto, H., Yamashita, S., Wu, X., Takahashi, H., Nishimura, J. et al. Decreased miR-340 expression in bone marrow is associated with liver metastasis of colorectal cancer. *Mol Cancer Ther.* 2014; doi: 10.1158/1535-7163.MCT-13-0571.
38. Inoue, A., Mizushima, T., Wu, X., Okuzaki, D., Kambara, N., Ishikawa, S. et al. miR-29b byproduct sequence exhibits potent tumour-suppressive activities via inhibition of NF- κ B signaling in KRAS-mutant colon cancer cells. *Mol Cancer Ther.* 2018; doi: 10.1158/1535-7163.MCT-17-0850.
39. Fukata T, Mizushima T, Nishimura J, Okuzaki D, Wu X, Yamamoto H, et al. The Supercarbonate Apatite-MicroRNA Complex Inhibits Dextran Sodium Sulfate-Induced Colitis. *Mol Ther Nucleic Acids.* 2018; doi: 10.1016/j.omtn.2018.07.007.
40. Morimoto Y, Mizushima T, Wu X, Okuzaki D, Yokoyama Y, Inoue A, et al. miR-4711-5p regulates cancer stemness and cell cycle progression via KLF5, MDM2 and TFDP1 in colon cancer cells. *Br J Cancer.* 2020; doi: 10.1038/s41416-020-0758-1.
41. Forterre A, Komuro H, Aminova S, Harada M. A Comprehensive Review of Cancer MicroRNA Therapeutic Delivery Strategies. *Cancers (Basel).* 2020; doi: 10.3390/cancers12071852.
42. Abd-Aziz N, Kamaruzman NI, Poh CL. Development of MicroRNAs as Potential Therapeutics against Cancer. *J Oncol.* 2020; doi: 10.1155/2020/8029721.
43. Merhautova J, Demlova R, Slaby O. MicroRNA-Based Therapy in Animal Models of Selected Gastrointestinal Cancers. *Front Pharmacol.* 2016; doi: 10.3389/fphar.2016.00329.
44. Takahashi RU, Prieto-Vila M, Kohama I, Ochiya T. Development of miRNA-based therapeutic approaches for cancer patients. *Cancer Sci.* 2019; doi: 10.1111/cas.13965.

45. Giuseppe Gagliardi and Charles F. Bellows. DCLK1 expression in gastrointestinal stem cells and neoplasia. *Journal of Cancer Therapeutics & Research*. 2012; doi: 10.7243/2049-7962-1-12.
46. Westphalen CB, Asfaha S, Hayakawa Y, Takemoto Y, Lukin DJ, Nuber AH, et al. Long-lived intestinal tuft cells serve as colon cancer-initiating cells. *J Clin Invest*. 2014; doi: 10.1172/JCI73434.
47. Westphalen CB, Takemoto Y, Tanaka T, Macchini M, Jiang Z, Renz BW, et al. Dclk1 defines quiescent pancreatic progenitors that promote injury-induced regeneration and tumorigenesis. *Cell Stem Cell*. 2016; doi: 10.1016/j.stem.2016.03.016.
48. Weygant N, Qu D, May R, Tierney RM, Berry WL, Zhao L, et al. DCLK1 is a broadly dysregulated target against epithelial-mesenchymal transition, focal adhesion, and stemness in clear cell renal carcinoma. *Oncotarget*. 2015; doi: 10.18632/oncotarget.3059.
49. Jiang D, Xiao C, Xian T, Wang L, Mao Y, Zhang J, Pang J. Association of doublecortin-like kinase 1 with tumor aggressiveness and poor biochemical recurrence-free survival in prostate cancer. *Oncotargets Ther*. 2018; doi: 10.2147/OTT.S157295.
50. Kantara C, O'Connell M, Sarkar S, Moya S, Ullrich R, Singh P. Curcumin promotes autophagic survival of a subset of colon cancer stem cells, which are ablated by DCLK1-siRNA. *Cancer Res*. 2014; doi: 10.1158/0008-5472.CAN-13-3536.
51. Ji D, Zhan T, Li M, Yao Y, Jia J, Yi H, et al. Enhancement of Sensitivity to Chemo/Radiation Therapy by Using miR-15b against DCLK1 in Colorectal Cancer. *Stem Cell Reports*. 2018; doi: 10.1016/j.stemcr.2018.10.015.
52. Abukhdeir AM, Park BH. P21 and p27: roles in carcinogenesis and drug resistance. *Expert Rev Mol Med*. 2008; doi: 10.1017/S1462399408000744.
53. Slingerland J, Pagano M. Regulation of the Cdk Inhibitor p27 and Its Deregulation in Cancer. *J Cell Physiol*. 2000; doi: 10.1002/(SICI)1097-4652(200004)183:1<10::AID-JCP2>3.0.CO;2-I.
54. LaBaer J, Garrett MD, Stevenson LF, Slingerland JM, Sandhu C, Chou HS, Fattaey A, Harlow E. New functional activities for the p21 family of CDK inhibitors. *Genes Dev*. 1997; doi: 10.1101/gad.11.7.847.
55. Chandrakesan P, May R, Qu D, Weygant N, Taylor VE, Li JD, et al. Dclk1+ small intestinal epithelial tuft cells display the hallmarks of quiescence and self-renewal. *Oncotarget*. 2015; doi: 10.18632/oncotarget.5129.
56. Adikrisna R., Tanaka S, Muramatsu S, Aihara A, Ban D, Ochiai T, et al. Identification of pancreatic cancer stem cells and selective toxicity of chemotherapeutic agents. *Gastroenterology*. 2012; doi: 10.1053/j.gastro.2012.03.054.
57. Rupaimoole R, Slack FJ. MicroRNA therapeutics: towards a new era for the management of cancer and other diseases. *Nat Rev Drug Discov*. 2017; doi: 10.1038/nrd.2016.246.

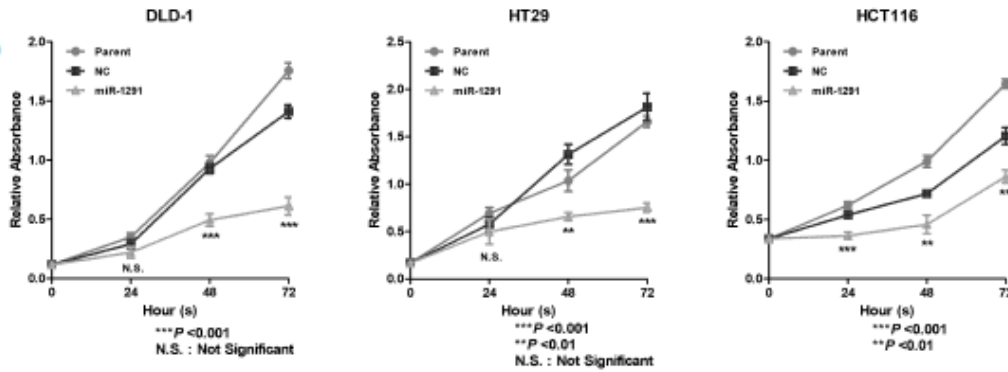
Figures

Figure 1

a



b



c

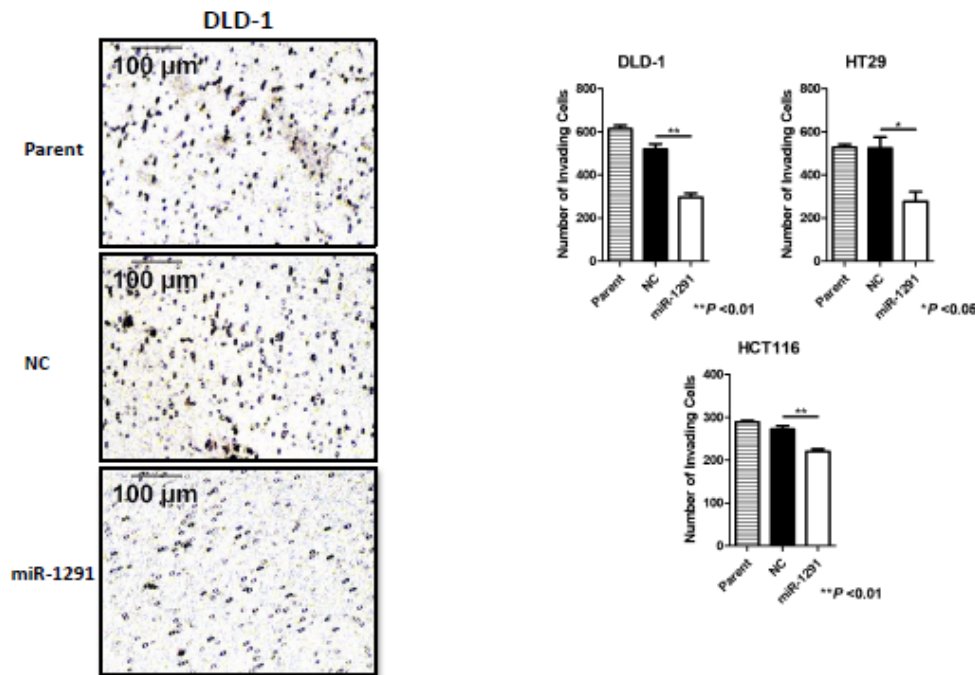


Figure 1

Inhibition of malignant properties of CRC cells by miR-1291. (a) MiR-1291 exhibited 1,000 to 5,000-fold higher overexpression than miR-NC after 4 or 24 hours of transfection. RNU6B was utilized as an endogenous control. (b) MiR-1291 significantly inhibited the proliferation of DLD-1, HT29, and HCT116 cells compared to miR-NC. The subtraction difference of absorbance between wavelength of 630 nm and 450 nm was used to determine cell number. (c) Invasion ability was significantly inhibited in DLD-1 cells

at 48 hours, HT29 cells at 72 hours, and HCT116 cells at 72 hours after transfection of miR-1291. Representative images are shown on the left. All experiments were performed more than three times. All data are presented as mean \pm SEM. * $P < 0.05$, ** $P < 0.01$, *** $P < 0.001$.

Figure 2

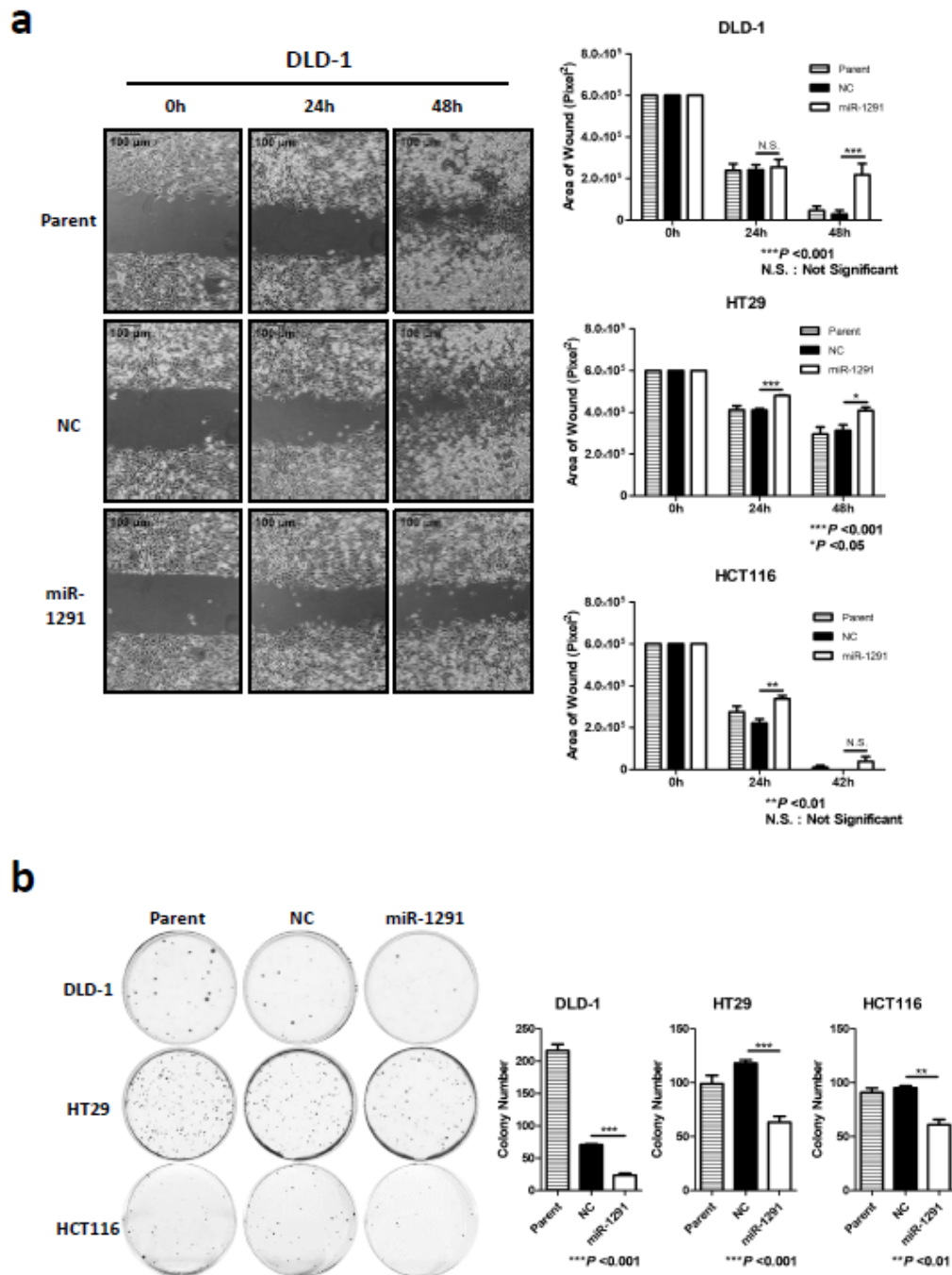


Figure 2

The effects of miR-1291 on cell migration and colony-forming ability in colorectal cancer cells. (a) Wound healing assay in DLD-1, HT29, and HCT116 cells treated with miR-NC or miR-1291. The wound area was

measured at the indicated times by ImageJ software. (b) The colony-forming ability was suppressed in DLD-1, HT29 and HCT116 cells, 10 days after transfection with miR-1291. All experiments were performed more than three times. All data are presented as mean \pm SEM. *P < 0.05, **P < 0.01, ***P < 0.001.

Figure 3

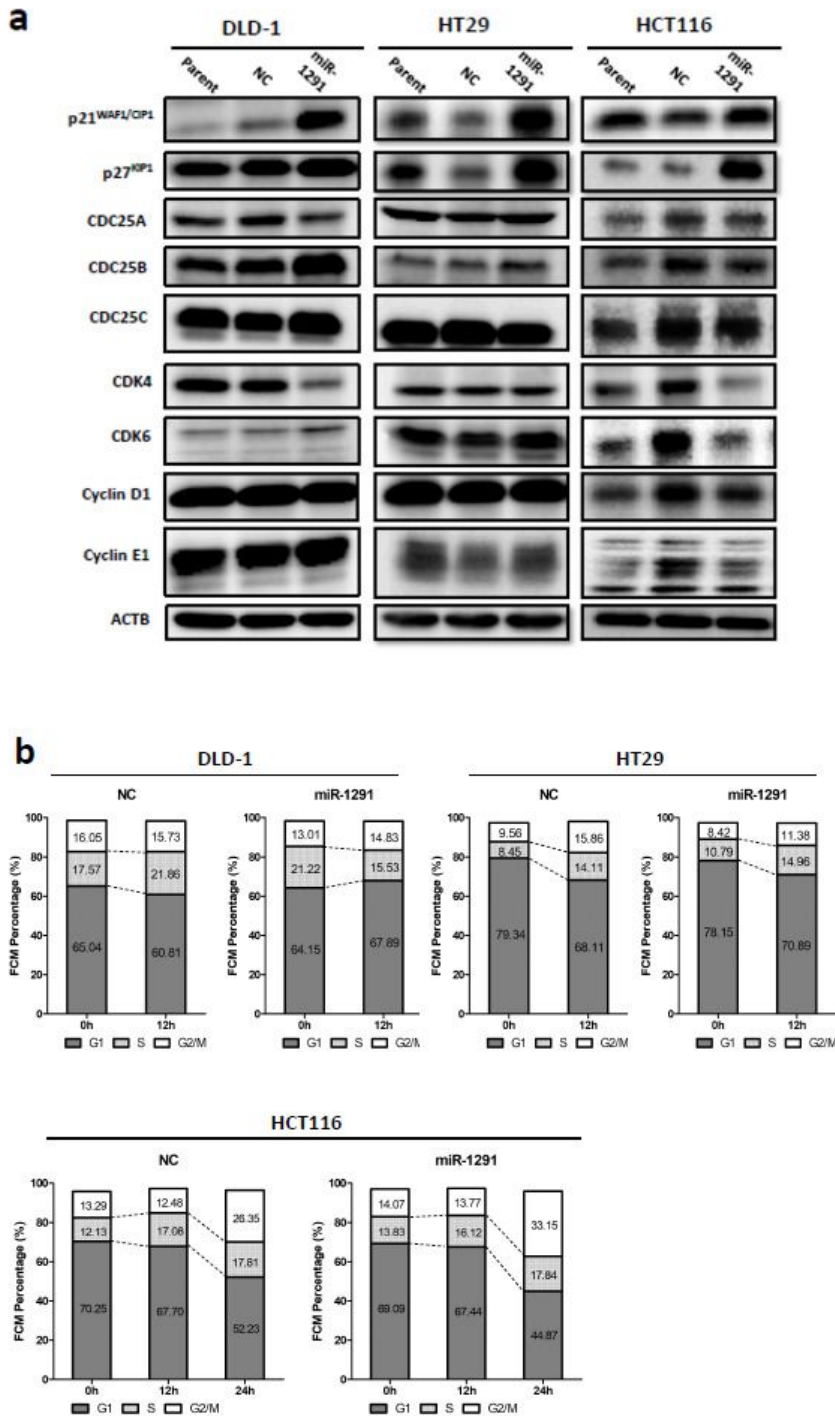


Figure 3

Cell cycle analysis. (a) The expression of cell cycle-related proteins was evaluated by Western blot analyses. Treatment of miR-1291 up-regulated the expression of p21WAF1/CIP1 and p27KIP1 in DLD-1, HT29 and HCT116 cells. MiR-1291 down-regulated the expression of CDK4 in DLD-1 cells and in HCT116 cells compared to miR-NC. ACTB was used as a loading control. (b) Cell cycle analyses by flow cytometry after treatment with miR-NC or miR-1291. MiR-1291 increased the percentage of cells in G1 phase in DLD-1 after 12 hours of addition of serum to the starved cells. MiR-1291 increased the percentage of cells in G2/M phase in HCT116 cells compared to miR-NC after 24 hours of addition of serum to the starved cells. Significant dysregulation was not found in HT29 in the miR-1291 group at G1, S, or G2/M phase compared to miR-NC group.

Figure 4

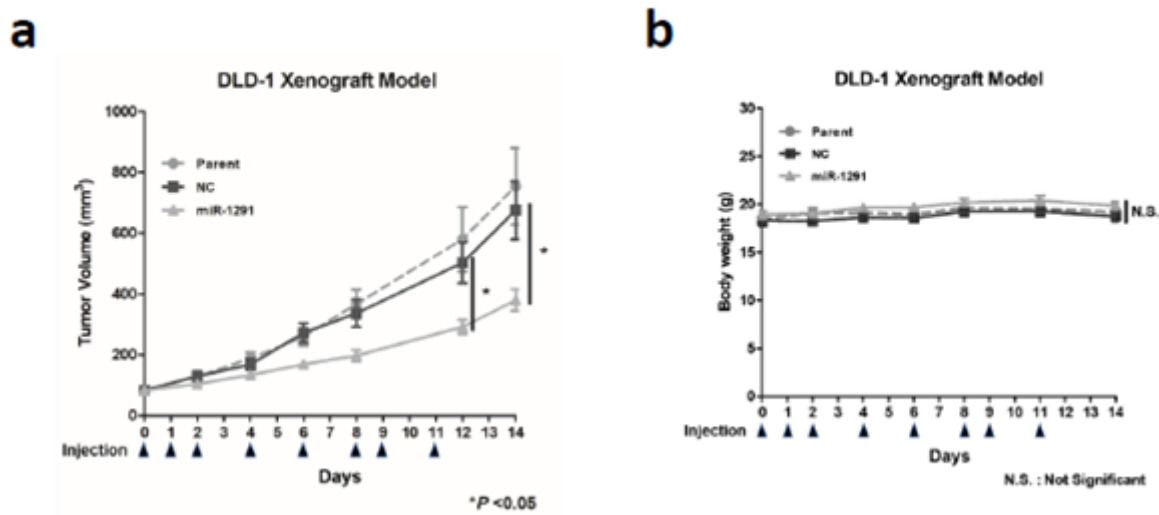


Figure 4

Systemic administration of formulated sCA-miR-1291 suppressed tumor growth in vivo. (a) Tumor volume. Tumor xenograft mouse models received intravenous administrations of miR-1291 or miR-NC using super carbonate apatite (sCA) as a vehicle on days 0, 1, 2, 4, 6, 8, 9, and 11 via a tail vein injection (arrows indicate days of injections). Each injection contained 40 μ g of formulated oligo. Data represent the mean \pm SEM. (P < 0.05, one-way ANOVA followed by Bonferroni's multiple comparisons test). (b) Body weight did not significantly differ between the groups.

Figure 5

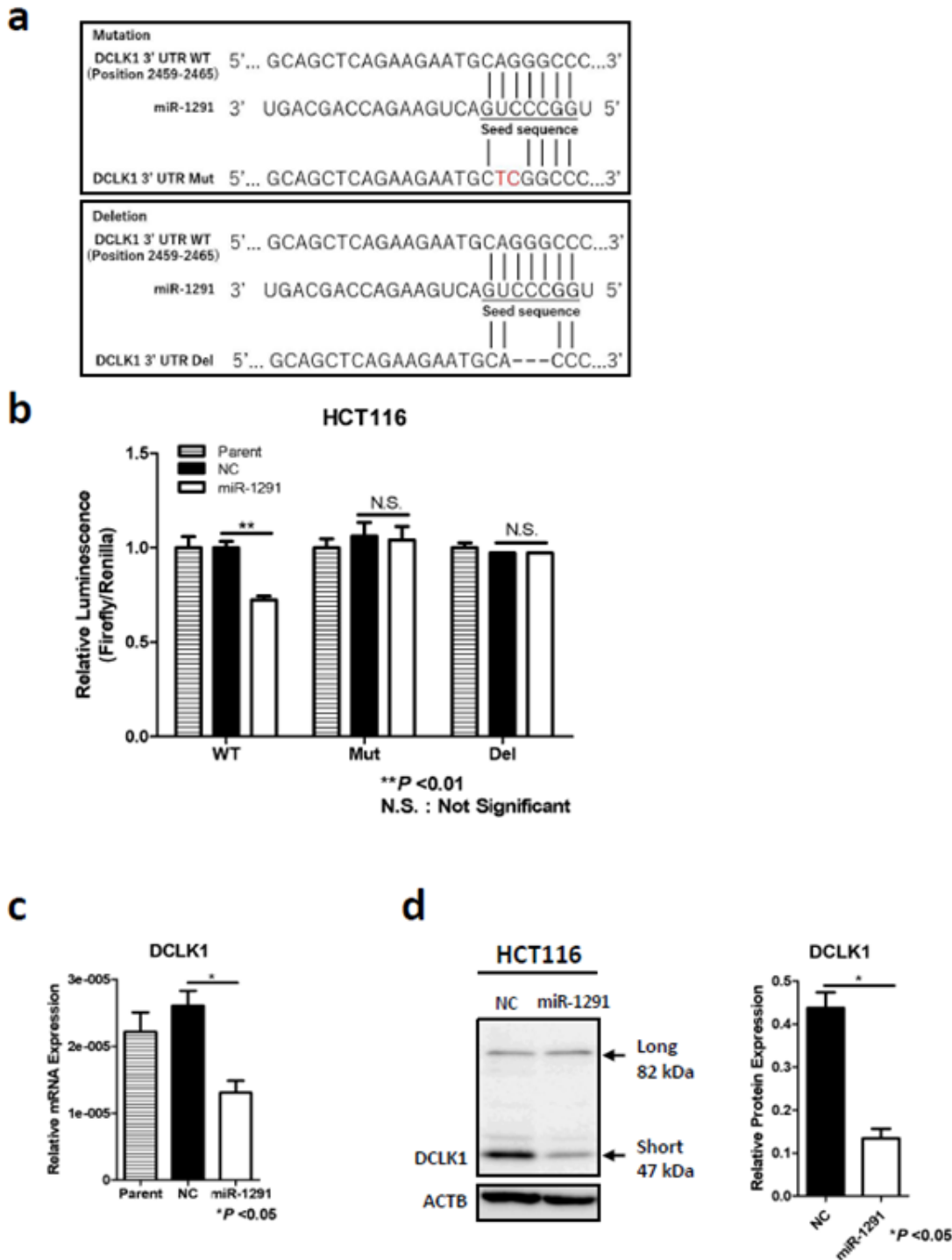


Figure 5

MiR-1291 directly targeted the 3' UTR of DCLK1 in HCT116. (a) Using NCBI (<https://www.ncbi.nlm.nih.gov/>), we identified a binding site at the position of 2459-2465 of the 3' UTR of DCLK1 mRNA that is complementary to the seed sequence of miR-1291 (WT). The binding sequence of DCLK1 was mutated by changing two nucleotides (Mut), or deleting three nucleotides (Del). (b) In HCT116 cells, transfection with miR-1291 significantly suppressed the relative luciferase activity of the

wild type plasmid of DCLK1 (WT, **P <0.01). On the other hand, no significant difference was noted with the mutated or deleted type plasmid of DCLK1 (Mut or Del). (c) The effect of miR-1291 on the expression of DCLK1 were assessed by qRT-PCR. MiR-1291 significantly inhibited the expression of DCLK1 mRNA in HCT116 cells. GAPDH was utilized as an endogenous control. (d) Western blot showed that miR-1291 decreased DCLK1 protein expression after 48 hours of transfection in HCT116 cells. ACTB was used as a loading control. Two independent experiments indicated that treatment with miR-1291 reduced the DCLK1 expression to 30.6% of that treated with miR-NC (*P <0.05).

Figure 6

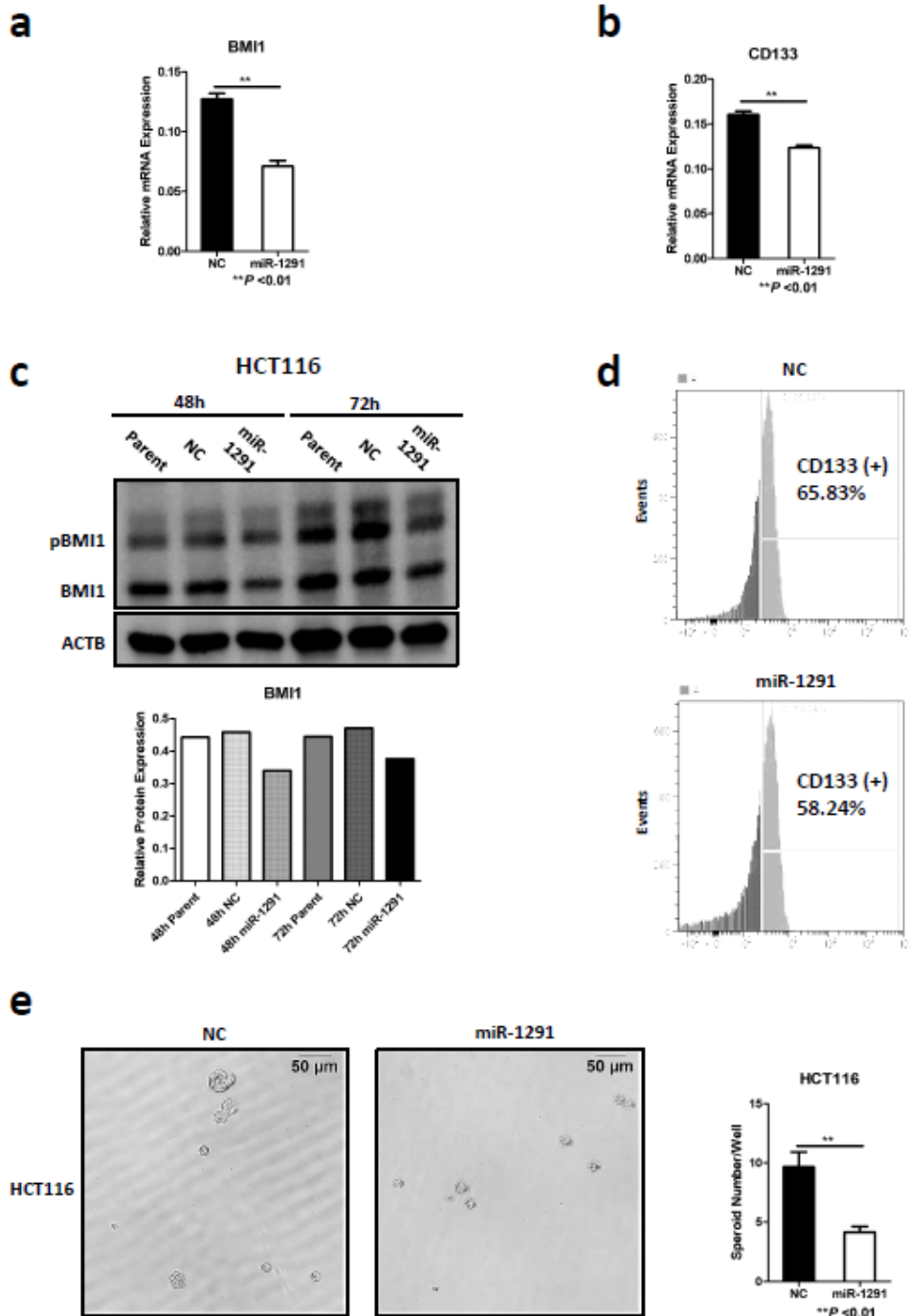


Figure 6

MiR-1291 suppressed the stemness of HCT116 cells. (a, b) QRT-PCR was performed to evaluate the stemness. The expression of stem cell markers BMI1 and CD133 was significantly decreased by miR-1291. GAPDH was utilized as an endogenous control. (c) MiR-1291 suppressed BMI1 protein expression after 48 and 72 hours of transfection compared to miR-NC. ACTB was used as a loading control. (d) Flow cytometry showed that the ratio of stem cell surface marker CD133 was decreased by miR-1291 compared to miR-NC. (e) The sphere formation ability was significantly suppressed in miR-1291 transfected HCT116 cells compared to miR-NC. The number of spheres $\geq 40 \mu\text{m}$ was counted 4 days after seeding. Representative images are shown on the left. In a, b, and e, the experiments were performed more than three times, and data are presented as mean \pm SEM. **P < 0.01.

Supplementary Files

This is a list of supplementary files associated with this preprint. Click to download.

- [Additionalfile1.pdf](#)
- [Additionalfile2.pdf](#)
- [Additionalfile3.pdf](#)
- [Additionalfile4.pdf](#)
- [Additionalfile5.pdf](#)
- [Additionalfile6.pdf](#)
- [Additionalfile7.pdf](#)